Large deformation properties of reconstituted Christchurch sand subjected to undrained cyclic torsional simple shear loadings

G. Chiaro, T. Kiyota & H. Miyamoto

Institute of Industrial Science, University of Tokyo, Japan

2015 NZSEE
Conference

ABSTRACT: Severe liquefaction was repeatedly observed during the 2010-2011 Christchurch earthquakes, particularly affecting deposits of fine sands and silty sands of recent fluvial or estuarine origin. The effects of liquefaction included major sliding of soil toward water bodies (i.e. lateral spreading) ranging from centimetres to several metres. In this paper, a series of undrained cyclic torsional shear tests were conducted to evaluate the liquefaction and extremely large deformation properties of Christchurch boiled sand. In these tests, the simple shear conditions were reproduced in order to apply realistic stress conditions that soils experience in the field during horizontal seismic shaking. Several hollow cylindrical medium dense specimens (D_r = 50%) were prepared by pluviation method, isotropically consolidated at an effective stress of 100 kPa and then cyclically sheared under undrained conditions up to 100% double amplitude shear strain (γ_{DA}). The cyclic strength at different levels of γ_{DA} of 7.5%, 15%, 30% and 60%, development of extremely large post-liquefaction deformation and shear strain localisation properties were assessed from the analysis of the effective stress paths and stress-strain responses. To reveal possible distinctiveness, the cyclic undrained behaviour of CHCH boiled sand was compared with that of Toyoura sand previously examined under similar testing conditions.

1 INTRODUCTION

In the period between September 2010 and December 2011, Christchurch (New Zealand) and its surroundings were hit by a series of strong earthquakes including six major events, all generated by local faults in proximity to the city (Fig. 1): 4 September 2010 (M_w = 7.1), 22 February 2011 (M_w = 6.2), 13 June 2011 (M_w = 5.3 and M_w = 6.0) and 23 December 2011 (M_w = 5.8 and M_w = 5.9) earthquakes (Cubranovski et al. 2012). Because of their strength and proximity to the city, the earthquakes caused tremendous physical damage and impacts on the people, natural and built environments of Christchurch. Re-liquefaction was extensively observed in many areas of the city. After the three major earthquakes (Sept. 2010, Feb. 2011 and June 2011), several members of the Japanese Geotechnical Society (JGS), including the second Author of this paper, visited the Christchurch damaged area in order to conduct liquefaction-induced damage surveys and geotechnical investigations (Kiyota et al. 2011; 2012).

The business area of Christchurch city is located about 8.5 km west of the coast line. A tortuous stream, named Avon River, flows through the central part of Christchurch city. Areas along the Avon River were reportedly inundated with boiled sand after each major earthquake (Cubranovski et al. 2012; Kiyota et al. 2011; 2012). During the geotechnical survey following the February 2011 earthquake, a sample of Christchurch Avonside boiled sand (hereafter referred simply as CHCH boiled sand) was collected from the Dallington area (Fig. 2) to conduct detailed laboratory investigations, which results are presented in this paper.

A series of undrained cyclic torsional shear tests were conducted on reconstituted specimens to evaluate the liquefaction and extremely large deformation properties of CHCH boiled sand. A number of hollow cylindrical specimens were prepared by pluviation method, isotropically consolidated at an effective stress of 100 kPa and then cyclically sheared under undrained conditions up to about 100% double amplitude shear strain (γ_{DA}). The cyclic strength at different levels of γ_{DA}, development of large

post-liquefaction deformation and shear strain localisation properties were assessed from the analysis of the effective stress paths and stress-strain responses.
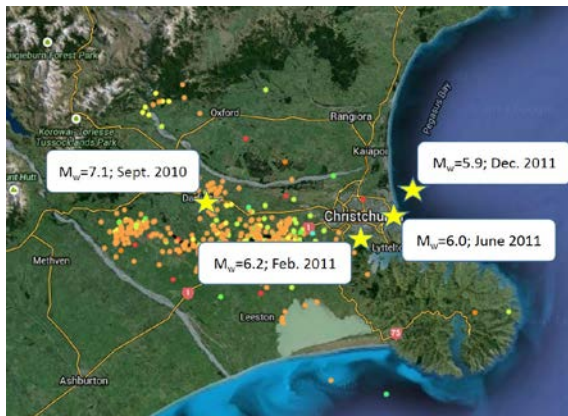

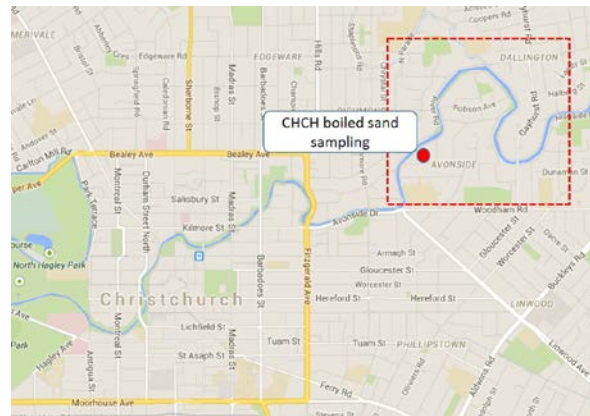Figure 1. Epicentres of major 2010-2011Christchurch earthquakes (adapted from Christchurch Quake Map).

Figure 2. Location of CHCH boiled sand sampling in Dallington.

2 TESTING PROCEDURE

2.1 Test apparatus

Torsional shear apparatus on hollow cylindrical specimen is recognized to be a good tool to properly evaluate liquefaction soil response (e.g. Tatsuoka et al. 1986). In particular, it offers the possibility to reproduce simple shear conditions, which are a close representation of field stress conditions during earthquakes. In this study, to reach extremely large torsional shear displacements, a fully automated torque loading apparatus on hollow cylindrical specimens (Fig. 3), developed in the Institute of Industrial Science, University of Tokyo (Kiyota et al. 2008), was employed. It is capable of achieving torsional γ_{DA} levels exceeding 100% by using a belt-driven torsional loading system that is connected to an AC servo motor through electro-magnetic clutches and a series of reduction gears. A two-component load cell, which is installed inside the pressure cell, was used to measure both the torque and the axial load components. Confining pressure obtained by the difference in pressure between the cell pressure and the pore water pressure was measured by a high capacity differential pressure transducer (HCDPT). To evaluate large torsional deformations, a potentiometer with a wire and a pulley was employed. In conducting cyclic shear tests, the specified shear stress amplitude was controlled by a computer, which monitors the outputs from the load cell, computes the shear stress (i.e. the measured shear stress was corrected for the effects of membrane force; Koseki et al. 2005) and controls the device accordingly.

2.2 Material and specimen preparation

All the tests were performed on CHCH sand (Fig. 4), which is boiled sand with non-plastic fines content (specific gravity, $G_s = 2.654$; maximum void ratio, $e_{max} = 1.081$; minimum void ratio, $e_{min} = 0.654$; and fines content under 75 μm, $F_c = 5\%$). As shown in Fig. 4, the particle size distribution curve for tested CHCH sand sample corresponds to the lower boundary in the range of values reported for this sand by Kiyota et al. (2011).

Several specimens with initial relative density of $D_{r100} = 50\%$ were prepared by air pluviation method (Table 1). To minimize the degree of inherent anisotropy in the radial direction of hollow cylindrical sand specimens, specimens preparation was carried out carefully by pouring the air-dried sand particles into a mould while moving radially the nozzle of the pluviator and at the same time circumferentially in alternative directions i.e. first in clock-wise and then anti clock-wise directions (De Silva et al. 2006). In addition, to achieve specimens with highly uniform density, the falling height was kept constant throughout the pluviation process. Also, to attain a high degree of saturation: (i)

firstly, the double vacuum method (Ampadu and Tatsuoka 1993) was employed; (ii) then, de-aired water was circulated into the specimens; and (iii) finally, a back pressure of 200 kPa was applied. A Skempton's B-value ≥ 0.97 was confirmed for all the tested specimens.

The hollow cylindrical specimens with initial dimensions of 150 mm in outer diameter, 90 mm in inner diameter and 300 mm in height, were then isotropically consolidated by increasing the effective stress state (p') up to 100 kPa (this value was chosen to enable ease of comparison with Toyoura sand specimens). Afterward, undrained cyclic torsional loading with shear stress constant amplitude (τ_{cyc} = 12-30 kPa) was applied at a constant shear strain rate of about 0.25 %/min. The loading direction was reversed when the amplitude of cyclic shear stress, which was corrected for the effect of membrane force, reached the target value. During the process of undrained cyclic torsional loading the vertical displacement of the top cap was prevented, with the aim to simulate as much as possible the simple shear condition. Note that, effects of membrane penetration due to excess pore water pressure generation on liquefaction resistance was not considered in this study, since their extents would be independent from the cyclic shear applied.
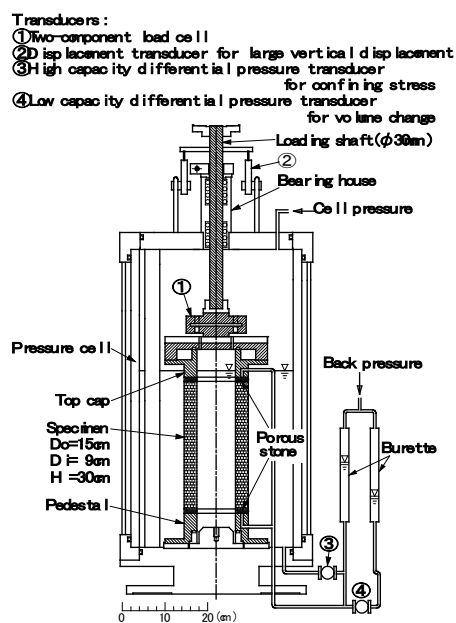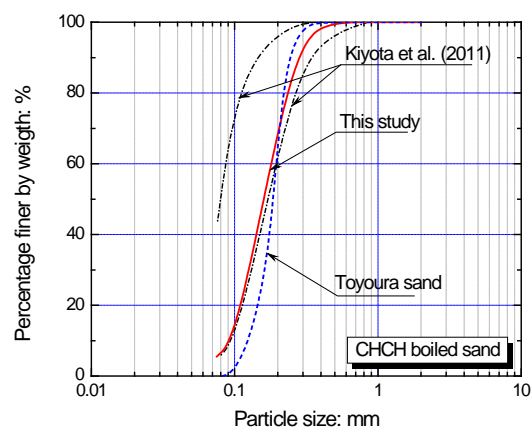

Figure 3. Torsional shear apparatus employed in this study (after Kiyota et al. 2008).

Sand	CHCH	Toyoura
Specific gravity, G_s	2.654	2.656
Max. void ratio, e_{max}	1.081	0.992
Min. void ratio, e_{min}	0.654	0.632
Fines content, F_c	5%	0.1%

Figure 4. Grain size distributions and index properties of CHCH boiled sand and Toyoura sand.

Table. 1 Testing conditions employed in this study.

Test	D_{r0} (%)	D_{r30} (%)	D_{r100} (%)	τ_{cyc} (kPa)	CSR	$N_{7.5}$	$\gamma_{L(SA)}$
TSCH-01	45.3	47.5	49.0	12	0.12	119	18.2%
TSCH-02	44.6	46.8	48.5	18	0.18	12.4	16.2%
TSCH-03	45.1	47.4	48.9	24	0.24	2.5	17.8%
TSCH-04	44.0	46.2	48.6	30	0.30	0.6	15.9%

Note: D_{r0}, D_{r30}, D_{r100} is the relative density measured at an effective mean stress of 0 kPa (i.e. initial condition), 30 kPa (i.e. pre-consolidation stage) and 100 kPa (i.e. end of isotropic consolidation), respectively; τ_{cyc} is the torsional cyclic shear stress; CSR is the cyclic stress ratio; $N_{7.5}$ is the number of loading cycle to cause a double amplitude shear strain of γ_{DA} = 7.5%; and $\gamma_{L(SA)}$ is the limiting shear strain single amplitude to cause shear strain localisation.

2.3 Correction of measured shear stress for torsional membrane force

In performing torsional shear tests on hollow cylindrical specimens, due to the presence of inner and outer membranes, the effect of torsional membrane force cannot be neglected (Koseki et al., 2005; among others). Membrane force becomes significantly important when shear strain reaches extremely high levels (Kiyota et al. 2008; Chiaro et al. 2012 and 2013). By employing the linear elasticity theory, which uses the Young's modulus of the membrane, the theoretical apparent shear stress (τ_m) induced by the inner and outer membranes can be evaluated as follows:

$$\tau_m = \frac{t_m E_m (r_{out}^3 + r_{inn}^3)\theta}{(r_{out}^3 - r_{inn}^3)H} \tag{1}$$

where θ is the rotational angle of the top cap detected by external potentiometer; H is the height of the specimen; r_{out} and r_{inn} are the outer and inner radii of the specimen; t_m and E_m are, respectively, the thickness (= 0.3 mm) and the Young's modulus (= 1470 kPa, Tatsuoka et al., 1986) of the membrane. To confirm the validity of Eqn. (1) in correcting for the effect of membrane force, two special tests were performed by filling water between the inner and outer membranes and shearing the water specimens monotonically and cyclically under undrained condition up to γ_{DA} = 100%. Figure 5 shows both experimental and theoretical relationships between shear strain and τ_m that is induced by the membranes due to torsional deformation. The deviation of the actual membrane deformation from the uniform cylindrical one that was theoretically assumed became larger with an increase in the strain level. Therefore, in this study, the shear stress was corrected for the effect of membrane force by employing the empirical hyperbolic correlation between γ and τ_m shown in Figure 5. For completeness, water specimen appearance before and during monotonic undrained shear tests is reported in Figures 5(b) and 5(c), respectively.
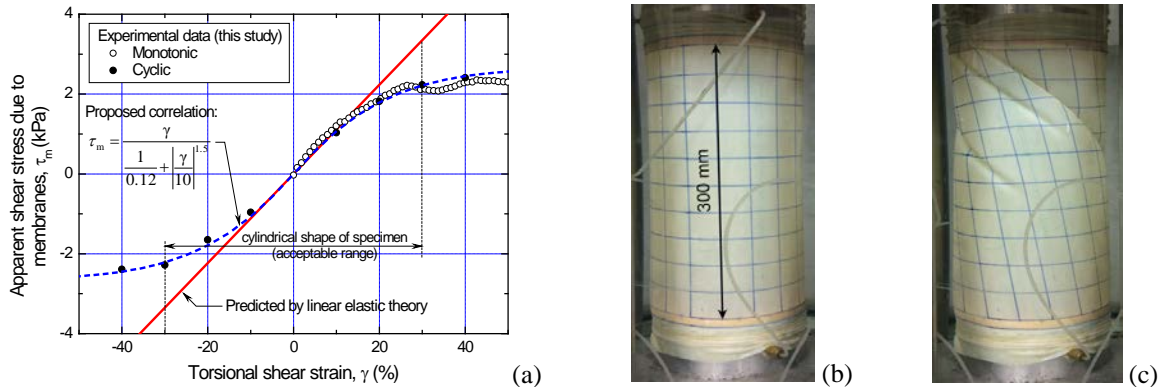

Figure 5. (a) Comparison between measured and calculated membrane force; (b) water specimen before monotonic shear test; and (c) water specimen deformation at $\gamma_{SA} \approx 25\%$ during monotonic shear test.

3 TEST RESULTS

3.1 Cyclic undrained response and liquefaction resistance

Figure 6 presents the cyclic undrained response of three CHCH sand specimens subjected to τ_{cyc} = 12, 18 and 30 kPa or a cyclic stress ratio (CSR = τ_{cyc}/p_0') of 0.12, 0.18, 0.30), respectively, in terms of effective stress paths and stress-strain relationships. Failure envelope and phase transformation line (PTL; Ishihara et al. 1975) are also reported for completeness.

As shown in Figure 6(a), due to the low value of CSR = 0.12, full liquefaction (p' = 0) was achieved after applying about 120 loading cycles. Subsequently, cyclic mobility was observed in the effective stress path, where following the failure envelope the effective mean stress recovered repeatedly. It was accompanied with a significant development of shear strain as evidenced by stress-strain relationship. Similar behaviour is observed when CSR = 0.18 is applied, with the exception that full liquefaction is achieved after 12 cycles of loading (Fig. 6(b)).

On the other hand, by applying a higher CSR = 0.30, the state of zero effective stress was achieved after applying just 1 cycle of loading (Figs 6(c)). Consequently, also large deformation was developed much quickly than the case of CSR = 0.12 and 0.18.
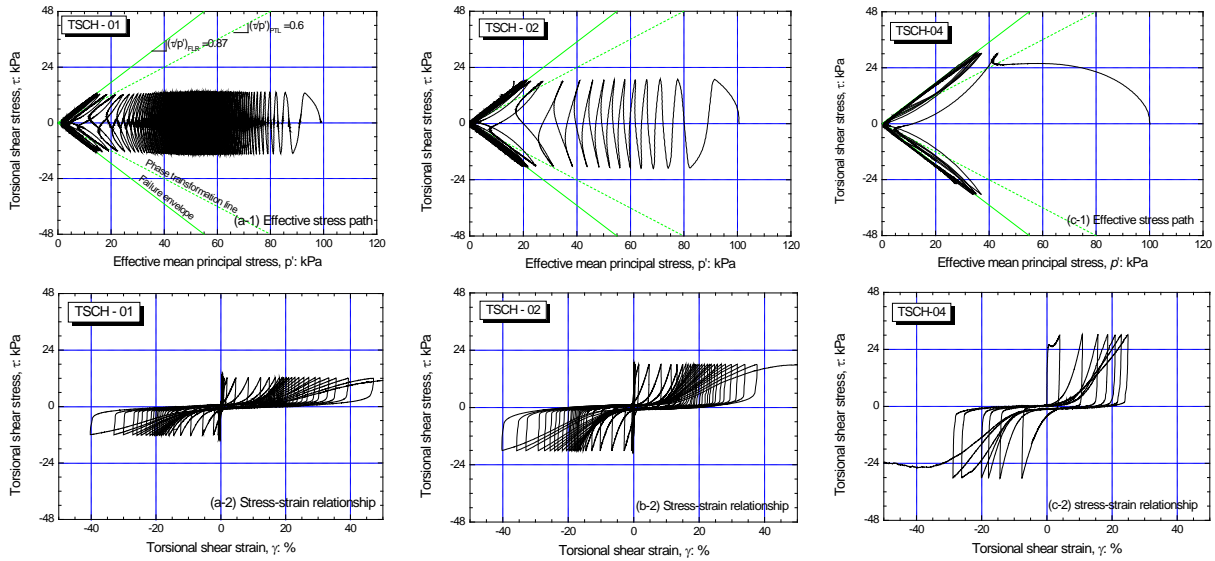

Figure 6. Test results for: (a) TSCH-01 (CSR=0.12); (b) TSCH-03 (CRS=0.18); and (c) TSCH-04 (CSR=0.30).

In Figure 7, a liquefaction resistance curve (defined as the number of cycles to cause γ_{DA} = 7.5%, which is equivalent to shear strain ε_{qDA} = 5% in triaxial tests) is plotted for CHCH sand and compared to that of Japanese Toyoura sand specimens. Despite the fact that CHCH sand has F_c = 5%, its liquefaction potential appears to be similar to that of Toyoura sand (F_c = 0.1 %) investigated under analogous testing conditions i.e. comparable density and effective mean stress and same specimen preparation method (Kiyota et al. 2008; Chiaro 2010).

3.2 Resistance against extremely large cyclic shear strain accumulation

Usually, the resistance against liquefaction or, more specifically, to cyclic strain accumulation is expressed as the number of cycles required to achieve certain level of deformation (from the initial configuration of the specimens) during cyclic loading. In the case of conventional triaxial tests, strain levels employed are usually limited to several percent to about 20%. In the present study, on the other hand, using torsional shear apparatus that was modified for enlarging the effective range of torsional displacement, the liquefaction characteristics could be obtained up to extremely large shear strain levels.

In Figure 8, the resistance to cyclic strain accumulation is plotted for CHCH sand as the number of cycles to cause γ_{DA} of 7.5%, 15%, 30% and 60%. It is clear that large deformation developed quickly for specimens that liquefied in just a few cycles of loading.

Cyclic resistance ratio at 15 cycles of loading (CRR$_{15}$) is a well-established parameter to judge the liquefaction potential of soils. Here, CRR$_{15}$ was evaluated for different γ_{DA} curves as displayed in Fig. 9a. Interestingly, it seems that CRR$_{15}$ increases gradually by following a linear trend, even after strain localisation. Significantly, compared to Toyoura sand, it is found that CHCH sand is stronger against extremely large deformation. The reasons behind this unpredicted behaviour are not fully understood yet. Therefore, aimed at clarifying this matter, additional laboratory analyses are currently being performed, including SEM scans. Due to time constrains, further results will be presented elsewhere.

It is important to mention that, the cyclic resistance value exceeding γ_{DA} 34% and 46% are only indicative since it is affected by strain localisation (Kiyota et al. 2008 and 2010; Chiaro et al. 2013) as described in the next section. This is because, after strain localisation occurrence at large strain levels, specimen deformation is non-uniform (Fig. 9b) i.e. usually in the top part of the specimen deformation diverges from the uniform one (here indicated by the red dotted line).
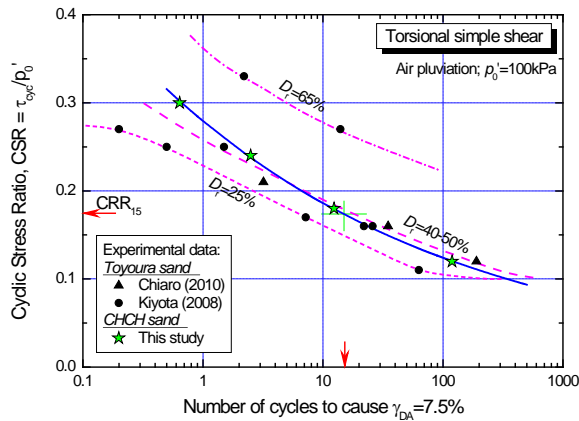
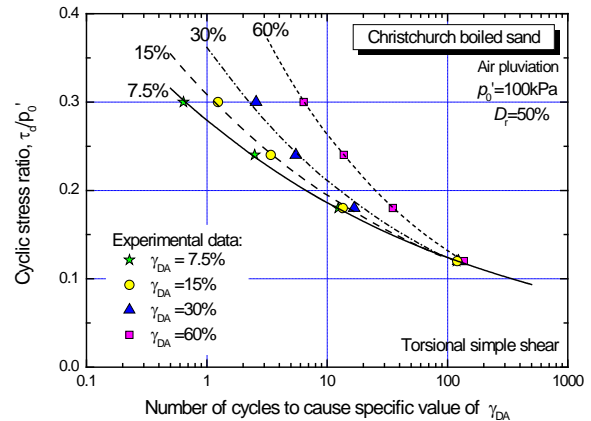**Figure 7. Liquefaction potential of CHCH sand compared to Toyoura sand.**

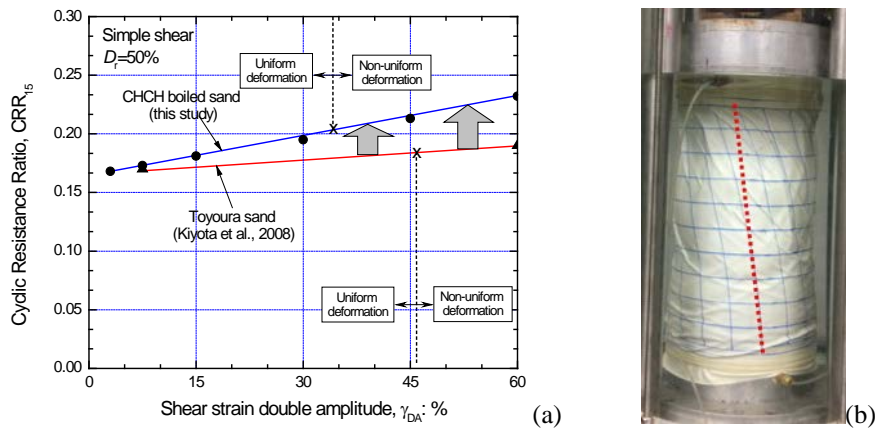**Figure 8. Resistance to extremely large cyclic shear strain accumulation.**

Figure 9. (a) Cyclic resistance ratio for different level of γ_{DA}; (b) typical non-uniform specimen deformation observed in liquefaction torsional shear tests on CHCH sand (photo refer to tests TSCH-01 at stage $\gamma_{DA} \approx 45\%$).

3.3 Development of large deformation and limit shear strain to cause strain localisation

In this study, the γ_{DA} value continued to increase up to approximately 100% (Fig. 10), which was the maximum capacity of the apparatus under employed test setting. Considerably, non-uniform deformation of the specimen or strain localisation was observed at higher strain levels (Fig. 9b). However, the beginning of such strain localisation could not be defined merely on the basis of visual observations. Thus, it was defined using the procedure described by Kiyota et al. (2008, 2010), by looking at the change in deviator stress and strain-softening behaviour of CHCH sand.

As suggested by Kiyota et al. (2008), the state at which the deviator stress q (calculated as the difference between vertical effective stress (σ_v') and radial effective stress (σ_r') i.e. $q = \sigma_v' - \sigma_r'$) drastically decreases during cyclic loading can be considered as the limiting state to initiate shear band (s) formation or strain localisation. In Figure 11, such state is defined as State A. Note that, due to the imposed simple shear conditions (i.e. vertical displacement of top cap was prevented), q was corrected for the effects of membrane force as proposed by Chiaro et al. (2013). It can be observed that, State A is usually followed by a repeating shear strain increment ($\Delta\gamma$) at State B (Fig. 12). Chiaro et al. (2013), observing the cyclic strain softening behaviour of Toyoura sand, confirmed that the state A is effectively the beginning of shear band formation into specimen and the State B is the beginning of residual tress state after completion of shear band formation. It is important to mention that originally Kiyota et al. (2008) defined the limit shear strain in terms of half of double amplitude shear strain $\gamma_{L(DA)}/2$, while Chiaro et al. (2013) recommended that double amplitude shear strain ($\gamma_{L(SA)}$) is a more

appropriate parameter when non-symmetric cyclic shear stress conditions are considered (e.g. an initial static shear in applied). Nevertheless, in the case of symmetric cyclic loading (i.e. zero static shear) $\gamma_{L(DA)}/2$ and $\gamma_{L(SA)}$ are well in accordance with each other Chiaro et al. (2013). Significantly, $\gamma_{L(SA)}$ (or $\gamma_{L(DA)}/2$) is independent from the CSR applied (Kiyota et al. 2008) and initial static shear Chiaro et al. (2013). In contrast, it decreases with density state (Kiyota et al. 2008).

Based on the above background and experimental findings, in this study, $\gamma_{L(SA)}$ was defined by looking at the change in q during cyclic loading (State A). Figure 13 compares $\gamma_{L(SA)}$ values obtained for CHCH sand with those evaluated for Toyoura sand by Kiyota et al. (2008) and Chiaro et al. (2013). It can be seen that, regardless of CSR applied, in the case of CHCH sand, $\gamma_{L(SA)} \approx 17\%$. Thus, it is slightly lower than that of Toyoura sand specimens prepared at similar density level, which is $\gamma_{L(SA)} \approx 23\%$.

Note that, Kiyota et al. (2010) proved that the limiting value to initiate strain localization observed in torsional shear tests (i.e. $\gamma_{L(SA)}$ or $\gamma_{L(DA)}/2$) are consistent with the maximum amounts of liquefied-induced ground displacement observed in relevant case studies by Hamada et al. (1988). According to Kiyota et al. (2010), as long as the liquefied sandy soils layer remains in uniform deformation under undrained condition, $\gamma_{L(SA)}$ may be used in estimating the maximum amount of liquefaction-induced ground displacement.
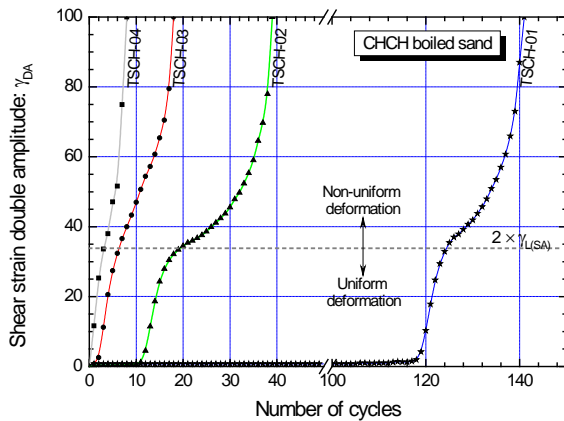

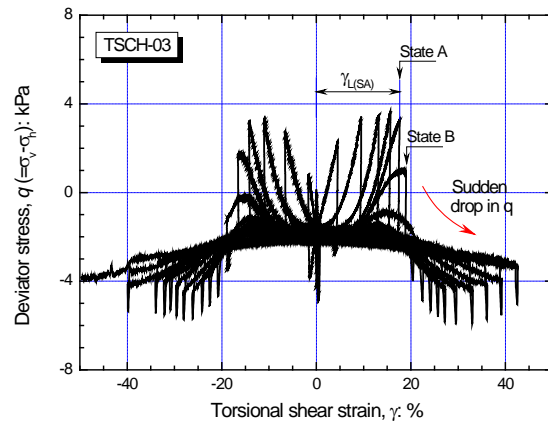**Figure 10. Large stain development observed during undrained cyclic torsional shear loading.**

Figure 11. Typical change in deviator stress properties undrained cyclic torsional shear loading.
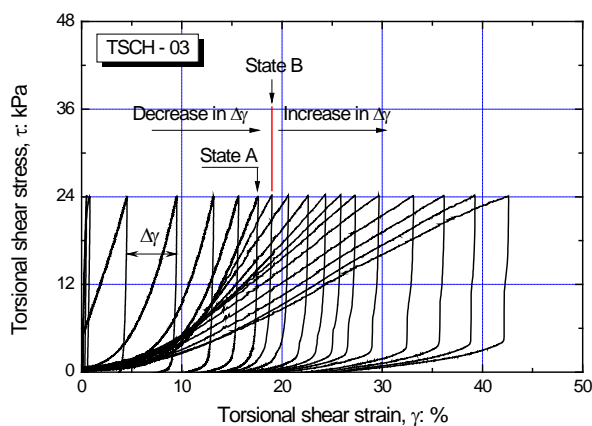

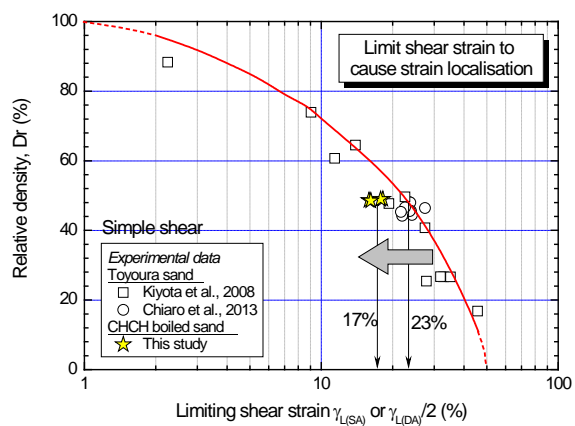**Figure 12. Change in shear strain properties during undrained cyclic torsional shear loading.**

Figure 13. Limiting shear strain to cause strain localisation in sandy soils.

4 CONCLUSIONS

To investigate the liquefaction and extremely large deformation properties of medium dense ($Dr \approx$ 50%) Christchurch boiled sand ($F_c = 5\%$), a series of hollow cylindrical cyclic torsional shear tests were carried out on specimens prepared by pluviation method, isotropically consolidated at an effective stress of 100 kPa and cyclically sheared up to 100% double amplitude shear strain (γ_{DA}). Interestingly, it was found that, when compared with Toyoura sand ($F_c = 0.1\%$), the liquefaction resistance defined at a $\gamma_{DA} = 7.5$ is similar for both sands, while the resistance to large cyclic shear strain ($\gamma_{DA} > 7.5$) of CHCH boiled sand is much higher than that of Toyoura sand. In addition, in the case of liquefied CHCH sand, strain localisation appears at a shear strain level of $\gamma_{L(SA)} \approx 17\%$, which is slightly lower than that of liquefied Toyoura sand ($\gamma_{L(SA)} \approx 23\%$) prepared at similar density state. The reasons behind this distinct behaviour of CHCH boiled sand are currently unidentified. Hence, aimed at clarifying this matter, additional laboratory analyses are now being carried out.

5 ACKNOWLEDGMENTS

6 REFERENCES

Ampadu, S.K. & Tatstuoka, F. 1993. Effects of setting method on the behavior of clays in triaxial compression from saturation to undrained shear, Soil*s and Foundations,* 33(2): 14-34.

Chiaro, G. 2010. Deformation properties of sand with initial static shear in undrained cyclic torsional shear tests and their modeling, *PhD Thesis*, Dept. of Civil Eng., University of Tokyo, Japan.

Chiaro, G., Kiyota, T. & Koseki, J. 2013. Strain localization characteristics of loose Toyoura sand in undrained cyclic torsional shear tests with initial static shear, *Soils and Foundations,* 53(1): 23-34.

Chiaro, G., Koseki, J. & Sato, T. 2012. Effects of initial static shear on liquefaction and large deformation properties of loose Toyoura sand in undrained cyclic torsional shear tests, *Soils and Foundations*, 52(1): 498-510.

Christchurch Quake Map: http://www.christchurchquakemap.co.nz/all

Cubrinovski, M., Henderson, D. & Bradley, B. 2012. Liquefaction impacts in residential areas in the 2010-2011 Christchurch Earthquakes. *Proc. of the International Symposium on Engineering Lessons Learned from the 2011 Great East Japan Earthquake*, Tokyo, Japan, 811-824.

De Silva, L.I.N., Koseki, J. & Sato, T. 2006. Effects of different pluviation techniques on deformation property of hollow cylinder sand specimens, *Proc. of the International Symposium on Geomechanics and Geotechnics of Particulate Media,* Ube, Yamaguchi, Japan, 29-33.

Hamada, M. Yasuda, S. & Wakamatsu, K. 1988. Case studies on liquefaction-induced permanent ground displacement, *Proc. of 1st Japan-US Workshop on Liquefaction, Large Ground Deformation and their Effects on Lifeline Facilities*, 3-21.

Ishihara, K., Tatsuoka, F. & Yasuda, S. 1975. Undrained deformation and liquefaction of sand under cyclic stresses, *Soils and Foundations,* 15(1): 29-44.

Kiyota, T., Koseki, J. & Sato, T. 2010. Comparison of liquefaction-induced ground deformation between results from undrained cyclic torsional shear tests and observations form previous model tests and case studies, *Soils and Foundations*, 50(3), 421-429.

Kiyota, T., Okamura, M., Toyota, H. & and Cubrinovski, M. 2011. Liquefaction-induced damage caused by the 2010 Darfield Earthquake, New Zealand, *ERS Bulletin*, IIS University of Tokyo, Japan, 44: 5-15.

Kiyota, T., Sato, T., Koseki, J. & Abadimaranad, M. 2008. Behavior of liquefied sands under extremely large strain levels in cyclic torsional shear tests, *Soils and Foundations*, 48(5): 727-739.

Kiyota, T., Yamada, S. & Hosono, Y. 2012. Repeated liquefaction observed during the 2010-2011 Canterbury Earthquakes, *ERS Bulletin*, IIS University of Tokyo, Japan, 45: 115-121.

Koseki, J., Yoshida, T. & Sato, T. 2005. Liquefaction properties of Toyoura sand in cyclic torsional shear tests under low confining stress, *Soils and Foundations*, 45(5): 103-113.

Tatsuoka, F., Sonoda, S., Hara, K., Fukushima S. & Pradhan, T. B. S. 1986. Failure and deformation of sand in torsional shear, *Soils and Foundations*, 26(4): 79-97.